Quantifying the Opportunity Limits of Automatic Residential Electric Load Shaping

Robert Cruickshank [1,2,*] **, Gregor Henze** [1,2] **, Rajagopalan Balaji** [1] **, Bri-Mathias Hodge** [2,3] **and Anthony Florita** [2]

[1] Department of Civil, Environmental and Architectural Engineering, University of Colorado Boulder, Boulder, CO 80309, USA

[2] National Renewable Energy Laboratory, Golden, CO 80401, USA

[3] Department of Electrical, Computer & Energy Engineering, University of Colorado Boulder, Boulder, CO 80309, USA

* Correspondence: robert.cruickshankiii@colorado.edu; Tel.: +1-703-568-8379

check for updates

Abstract: Electric utility residential demand response programs typically reduce load a few times a year during periods of peak energy use. In the future, utilities and consumers may monetarily and environmentally benefit from continuously shaping load by alternatively encouraging or discouraging the use of electricity. One way to shape load and introduce elasticity is to broadcast forecasts of dynamic electricity prices that orchestrate electricity supply and demand in order to maximize the efficiency of conventional generation and the use of renewable resources including wind and solar energy. A binary control algorithm that influences the on and off states of end uses was developed and applied to empirical time series data to estimate price-based instantaneous opportunities for shedding and adding electric load. To overcome the limitations of traditional stochastic methods in quantifying diverse, non-Gaussian, non-stationary distributions of observed appliance behaviour, recent developments in wavelet-based analysis were applied to capture and simulate time-frequency domain behaviour. The performance of autoregressive and spectral reconstruction methods was compared, with phase reconstruction providing the best simulation ensembles. Results show spatiotemporal differences in the amount of load that can be shed and added, which suggest further investigation is warranted in estimating the benefits anticipated from the wide-scale deployment of continuous automatic residential load shaping. Empirical data and documented software code are included to assist in reproducing and extending this work.

Keywords: electric load modeling; demand response; price-response; spectral representation

1. Introduction

Residential demand response programs typically are implemented as utility-initiated, infrequent, short-duration deferrals of peak electricity usage through direct load control. In direct load control, customers allow their utility to remotely turn off appliances such as air conditioning and water heating—a few times a year—for a credit on their electric bill [1]. Despite the promise of load management through supervisory control of the Internet of Things (IoT), direct load control has remained the primary form of residential demand response for several decades [1,2]. However, direct load control was never designed to shed and add load to accommodate the ebb and flow of wind and solar energy. As an alternative to direct load control, automatic residential load shaping (ARLS) is explored as a load elasticity solution for maximizing the system-wide efficiency of electric power generation via intraday control of IoT devices [3] while meeting the needs and comfort preferences of consumers.

To minimize consumer cost of electricity, an increasing number of smart homes with IoT devices can transition from an autonomous to an orchestrated operation that shapes load to favor energy from lower-cost wind and solar generation and higher efficiency conventional generation. Today, loads are typically created by controllers that are based on fixed temperature or battery charging setpoints; as such, these loads are considered inelastic in time. In the future, Internet-connected loads such as heating, ventilation and air conditioning (HVAC) systems, refrigerators, freezers, domestic hot water (DHW) heaters, and batteries could receive forecast dynamic pricing of electricity [4] or other load shaping signals that introduce elasticity by allowing each to choose monetarily or environmentally advantageous times to add or shed load. For example, changes in pricing could be used to update setpoints, allowing IoT devices to implement operating strategies that minimize their cost of operation. In doing so, instead of the traditional electrical supply-meets-demand relationship, load shaping would be necessary in modulating elastic demand to leverage the cheapest sources and times of supply, thereby reducing thermal and greenhouse gas emissions from power plants while maximizing the usage of clean energy from renewable energy sources (RES). Furthermore, understanding the limits of load shed and add opportunities would inform the design of generation, transmission, buildings, and appliances in support of joint optimization of power production and electric load. For example, understanding the opportunity limits of ARLS may support the business case for hot water heaters and freezers to have increased thermal storage in order to maximize usage of wind and solar energy.

Modeling diverse energy use in residential loads can be problematic due to different models and ages of appliances [5]. Furthermore, residential loads often exhibit non-stationary energy use behaviour based on the unknown needs of occupants that may vary by the hour of the day, the day of the week, seasons, shopping schedules, and home cleaning schedules [6]. Non-stationary energy usage is difficult to quantify and simulate using traditional stochastic methods [7]. Preserving energy usage diversity can raise the fidelity of electric load models [4], allowing for more realistic simulation of the generation-to-load system-level response to pricing signals intended to shape residential demand. The role of system-level response gains importance in the application of increasing penetration of wind and solar RES [8–10].

Despite aging components and ever-increasing complexity, the evolving electric grid is highly reliable [11] though expensive to operate. In order to accommodate spatiotemporal changes in inelastic load along with variable and uncertain generation from RES, expensive marginal generation and reserve capacity are kept online and dispatched as needed [12]. To address environmental concerns and reduce the cost of generation, RES are becoming more prevalent [13] with an increasing number of cities, counties, states, and nations aspiring to high RES penetrations, some as high as 100% by 2050 [14]. Because RES are less forecastable and some are not dispatchable at all, there is a growing need for creating load elasticity that can accommodate increasingly volatile supply-demand mismatches.

This paper extends the investigations of the opportunity limits of ARLS [6] by quantifying load shaping opportunities and uncertainty across a varying number of homes and by applying recent developments in spectral simulation techniques from hydrology research. The spectral techniques are applied to solve the research question of quantifying and simulating instantaneous load shaping opportunities based on empirical data that reflect non-stationary appliance energy usage. The novelty of this work is the use of empirical in situ measurements as seeds for the creation and scaling of realistically diverse appliance demand profiles. Simulation of diversity in energy consumption—without *a priori* knowledge of specific appliance and usage characteristics—is significant as it provides building blocks for mimicking energy usage behaviour in a subdivision of homes for demand response planning and operational decision making. Section 2 presents a review of the literature. Section 3 describes the methodology. Section 4 discusses results, and Section 5 presents conclusions and outlook for future work.

2. Literature Review

Demand response literature was reviewed with the goal of identifying: (1) Recent developments in approaches to system-level price-response involving time-elastic end uses, (2) Modeling gaps in price-response mechanisms, (3) Human behavioural issues related price-response, and (4) Recommendations for future price-response research. Darby and McKenna [15] suggested that new demand response measures will be needed to shape load throughout the day. Likewise, based on recent experience in the United States and Europe [16,17], the net load after renewable generation (i.e., the total load less the RES generation) is significantly less predictable and more volatile and will need to be smoothed by demand response. Results of elasticity experiments by McKenna and Keane found the introduction of dynamic pricing reduced the diversity of demand and increased coincidental response by promoting the same characteristics of response among (Internet-connected) automated appliances [4].

A review of 117 residential electricity demand models [18] indicated significant variability across households and raised questions as to whether high-resolution stochastic modeling approaches provide an adequate representation of the real world load characteristics of appliances. Adequate representation is important given the massive body of model-based time-of-use and real-time pricing assessments that have been used to address various aspects of residential demand response behaviour. Furthermore, coupling the inherent limits of stochastic models along with diversity being reduced by pricing based response [4] further raises the concern for adequately modeling appliance behaviour.

In a study of the most comprehensive data set of metered electricity demand in the United Kingdom, empirical and simulated consumption data were analyzed on an aggregated annual basis [5]. The comparison used qualitative and quantitative methods between simulated and metered data sets, and discrepancies were found in overall household and individual appliance electricity consumption, where non-normality of the data was apparent. A kernel density estimate of the distribution of empirical annual consumption data revealed the existence of a trimodal underlying distribution, which makes intuitive sense at both the appliance and household level. For example, around the world, electric hot water heaters are (1) most often in standby mode drawing no power, (2) are less often in short recharge mode when recovering from standby losses or light-use activities such as washing hands, or (3) are in long recharge mode when recovering from high-use activities such as dish and clothes washing. A different study, aggregating large numbers of residential appliances for demand response applications, used a methodology based on a multi-class queuing system, where each class represented demand blocks of a specific power level, time duration, and a service delay requirement. The model minimized the cost of the appliances' aggregated power consumption under day-ahead pricing [19]. A shortcoming of the model was the randomization of demand data from a single consumer to represent the demand behaviour of 1000 consumers.

Overall, the review of the demand response literature suggested a scarcity of system-level generation-to-load models of price-response and an abundance of subsystem models with unspecified or limited spatiotemporal resolutions. Furthermore, the review revealed the need for bottom-up, data-based, system-level models to simulate the impact of optimal demand response strategies in maximizing efficient usage of thermal and RES generation. Also needed are top-down policy measures that provide appropriate demand response incentives.

3. Methodology

3.1. Data and Methods

The field data analyzed in this study are from the Residential Building Stock Analysis (NEEA RBSA): Metering Study, performed by the Northwest Energy Efficiency Alliance [20]. The data are from a random sample of real homes in WA, OR, ID, and Western MT that are representative of dwellings in the Northwest of the United States. The NEEA RBSA encompassed 29 months of energy usage in 15-min observations of single-family homes, and data readings were 90.5% available over

this period. Observations included total per residence electricity usage at the service entrance along with up to 25 individually measured loads per home that were acquired and reported separately, including various types of HVAC systems, appliances, lighting, entertainment, home office, and plug loads. The study [21] reported the energy use of 101 homes including the loads therein. In particular, the thermostatically controlled load (TCL) appliance data revealed how each device could provide ARLS capability. The TCL energy usage per interval allowed for the creation of detailed load shapes that provided insights to variable whole-house load.

The NEEA RBSA data captured the diversity in energy usage among homes and appliances likely due to variations in building size and construction, numbers of building occupants, occupant behaviors, and age of appliances. A continuum of short to long appliance run times was evident, reflecting the possibility that sickly or high-use appliances, some which operated nearly continuously, would not be able to participate in ARLS. Extreme care regarding data accuracy was used during the extraction, transformation, and loading of observations. Some observations were missing timestamps, some were out of the range of possible behavior, e.g, orders of magnitude too large or negative, and other observations were completely missing. Data anomalies raised questions about potential gaps or errors in acquisition, along with the possibility that some appliances, such as a secondary refrigerator or freezer, were intentionally turned off for days, weeks, or months. Energy units of kWh/15-min are referenced in this study due to the unavailability of instantaneous power measurements.

The colored bars in Figure 1 depict when an appliance was operating. Individual bar width is 15-min, and bar height denotes the kWh of electricity used in 15-min. A large colored region indicates a long run time, e.g., a refrigerator operating for an extended period after being opened or refilled with groceries.
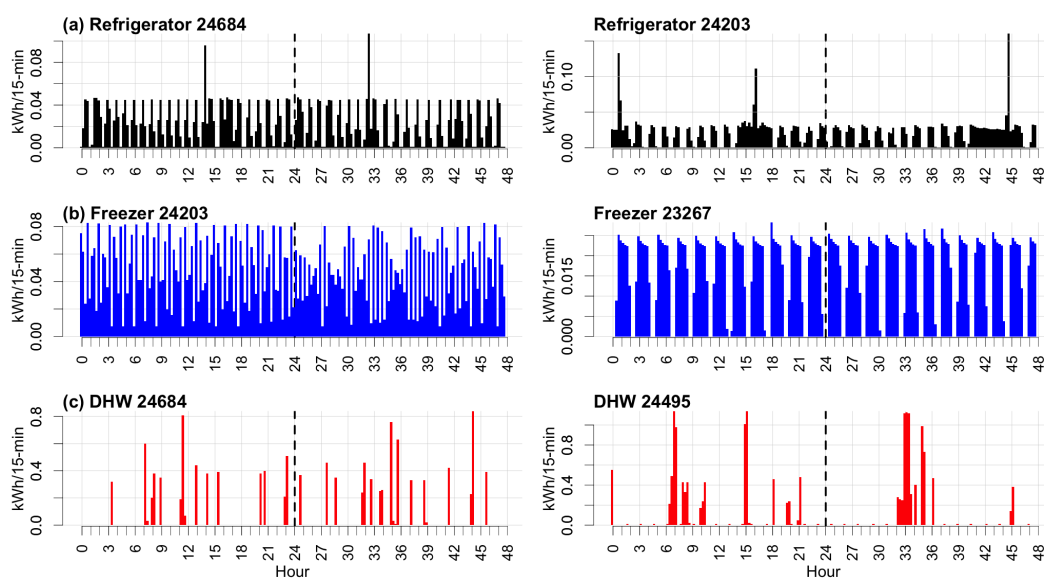

Figure 1. Energy usage of TCL appliances on 3–4 July 2012, showing kWh per 15-min interval. House numbers appear after appliance names and vertical dashed lines separate days. Note diversity in energy usage along axes: (**a**) two refrigerators, the one at right with a long run times in evenings and higher peak use; (**b**) two freezers, the one at right with nearly symmetric run times and lower peak use; and (**c**) two DHW heaters with typically low run times, the one at right with higher peaks.

Distributional statistics for NEEA RBSA TCL appliances were calculated and visualized using stochastic and spectral methods. Next, a binary model of conditional operation was developed to accommodate diversity in appliance energy consumption related to duration of use, frequency of use, and start time. Lastly, empirical data were simulated, and the probability density functions (PDFs) of resulting ensembles were compared to observations.

3.2. Modeling TCL Behaviour Using NEEA RBSA Data

To capture the diversity in energy usage, NERA RBSA TCL appliances were considered as contributors to desirable load increases or decreases based upon the on or off state of each over time. Load shaping opportunities were estimated throughout the day wherein TCL appliances were assumed to have Internet connectivity and the ability to change setpoints automatically to execute financially beneficial on and off choices during periods of low and high energy costs. An extreme illustrative case assumed contiguous non-overlapping temperature control setpoints for an electric DHW heater wherein the on state or off state of the device was used to estimate the instantaneous opportunity to increase or decrease load given an electricity price change. To simplify calculation of the potential for load shaping, it was further assumed that TCLs always operated within their control differential dead band as depicted in Table 1.

Table 1. Sample DHW heater non-overlapping setpoints. The 'Not modeled' entries reflect model constraints that limit operation between 120 and 130 F inclusive.

Temp. F	High $/kWh	Low $/kWh
131 and above	Not modeled	Not modeled
130	Always OFF	Turn Off
129	Always OFF	Stay ON
128	Always OFF	Stay ON
127	Always OFF	Stay ON
126	Always OFF	Stay ON
125	Turn OFF	Turn ON
124	Stay ON	Always OFF
123	Stay ON	Always OFF
122	Stay ON	Always OFF
121	Stay ON	Always OFF
120	Turn ON	Always OFF
119 and below	Not modeled	Not modeled

When the electricity price changed, from low to high, or high to low, TCL appliances reacted as described in Table 1. This state-based logic was replicated across all TCL appliances to produce estimates of Load Add and Load Shed opportunities in a time series that was summed within houses and across houses, without regard for phenomena such as the inefficiency of preheating or the impacts of energy rebound. Ideally, load shed and add would be expressed in units of power (kW). That said, only units of energy (kWh) were available in the RBSA Metering study.

At any instant in time, appliances were either off or on. Looking forward over n time steps of the energy usage of an individual appliance, a maximum load, L_{max}, was determined. At any time, t, the above logic estimated the load shed or add opportunity, OP. Given a high electricity price, an off appliance was given the incentive to turn on with a low price of electricity, which resulted in adding load, L_{add}, based on L_{max}, as in:

$$L_{add}^{appliance} = OP_{add\ load}^{OFF\ appliance} = L_{max(t,t+n)}^{appliance} \tag{1}$$

Given a low electricity price, an appliance with a load, L_t, was given the incentive to turn off with a high electricity price, which resulted in load shedding, L_{shed}, equal to negative L_t, as in:

$$L_{shed}^{appliance} = OP_{shed\ load}^{ON\ appliance} = -L_t^{appliance} \tag{2}$$

As modeled, if an appliance had partial load, then load addition was not applied, e.g., if L_t was less than *Lmax*.

Summing across TCL appliances per home yielded the lower and upper limits of load that could be shed or added as in (3) and (4):

$$L_{add}^{home} = \sum_{TCL\ appliances} L_{add}^{appliance} \tag{3}$$

$$L_{shed}^{home} = \sum_{TCL\ appliances} L_{shed}^{appliance} \tag{4}$$

Summing across homes yielded the lower and upper limits of load that could be shed or added as in (5) and (6):

$$L_{add}^{homes} = \sum_{homes} L_{add}^{home} \tag{5}$$

$$L_{shed}^{homes} = \sum_{homes} L_{shed}^{home} \tag{6}$$

In simplifying (1) through (6), the duty cycle, DC, quantified the on and off behaviour of a TCL appliance over any period. The DC described the behaviour of appliances with intermittent as opposed to continuous operation. The DC is the ratio of the appliance on time divided by the total applaince on and off time, as in:

$$DC_{t,t+n} = (ON\ time)_{t,t+n} / (total\ time)_{t,t+n} \tag{7}$$

In any period, appliances with a low DC had few opportunities to shed load as they were most likely already off. Likewise, somewhat counter-intuitively, a low duty cycle indicated many opportunities to add load, albeit for perhaps only a short duration. Conversely, a high duty cycle indicated a low opportunity to add load and a high opportunity to shed load, as in (8) and (9):

$$OP_{t,t+n}^{appliance\ add\ load} = 1 - DC_{t,t+n}^{appliance} \tag{8}$$

$$OP_{t,t+n}^{appliance\ shed\ load} = DC_{t,t+n}^{appliance} \tag{9}$$

Opportunities to shed and add load were summed across TCL appliances and then across homes as in (3)–(6) to yield estimates of the *instantaneous* downward and upward load-shaping opportunities. It is crucial to note that after a load decrease or increase event, the future operation of a TCL appliance has new constraints, e.g., due to comfort requirements, load add or shed cannot be shed or added continuously. Out of scope of this paper, though analyzed in related work, are the length, periodicity, and resulting load shed and add opportunities after appliances participate in a load increase or decrease event [22].

3.3. Scaling Up the NEEA RBSA Dataset

Diverse profiles from thousands of homes are required for the future application of this work involving the joint optimization of generation and load. In simulating ensembles of synthetic appliance data, spectral decomposition and reconstruction were used [23] to preserve the observed diversity in energy use. Spectral methods captured the non-normal, non-stationary energy usage of appliances and met the goal of specifying realistic probability distribution functions.

As summarized by [7], the application of traditional stochastic methods may fail to capture significant spectral properties. For example, measures such as mean, variance, and skew may fail to reproduce non-stationary behaviour in the observed data. Failure to capture spectral properties can lead to estimates that do not reflect the diversity of the load. As such, three variants of the wavelet auto-regressive method (WARM) [7] were compared in their ability to capture and recreate diverse energy usage of appliances.

As a first step, the TCL appliance energy usage observations were decomposed via continuous wavelet transform as depicted in Figure 2. Components were identified based on peaks in the global

(time-averaged) wavelet spectrum. The approach decomposed each time series of observations into different components at multiple frequencies using the wavelet transform; this provided the power, or variance, of the original observed behavior in both the time and frequency domains.
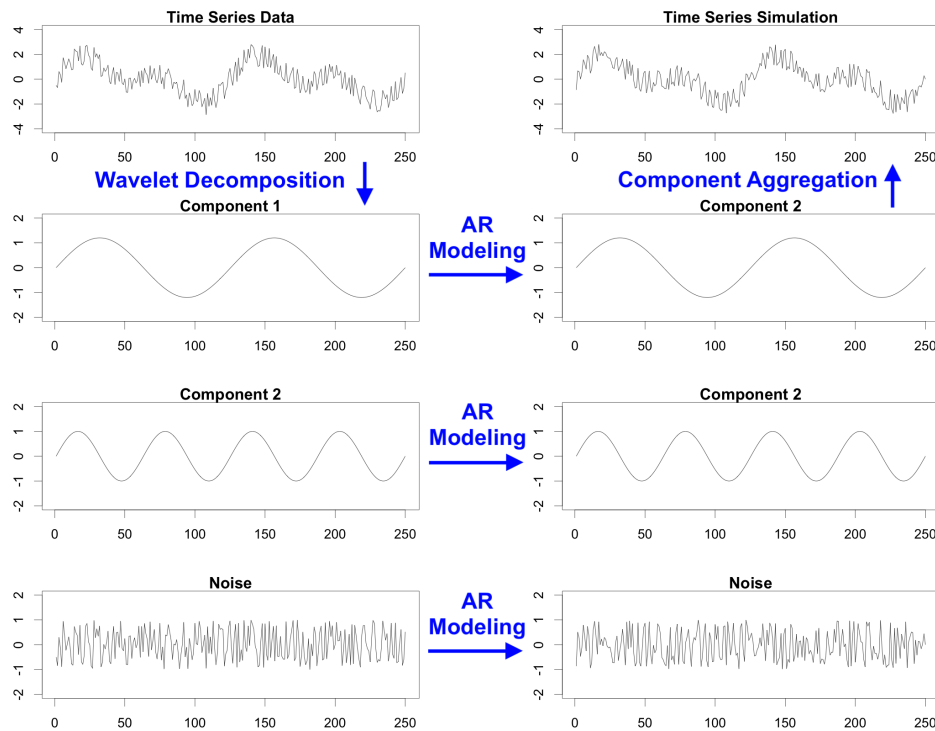

Figure 2. Example diagram of wavelet decomposition and aggregation using the enhanced WARM. Whereas the standard Fourier transform is localized in frequency, wavelets are localized in both frequency and time.

For a time series, x_t, the continuous wavelet transform was defined as:

$$X(a, b) = a^{1/2} \int_{-\infty}^{\infty} x_t \phi^* \left(\frac{t - b}{a} \right) dt \tag{10}$$

where *a* was a scale parameter (2 * dt = 30 min), $\phi*$ was the wavelet function and *b* was the shift parameter (1 * dt = 15 min) [24]. The * denotes a complex conjugate. The Morlet wavelet was a reasonable first choice in wavelet analysis, was most often applied by others with success, and was given by:

$$\phi(\eta) = \pi^{-1/4} exp(i\omega_o \eta) exp\left(-\frac{n^2}{2} \right) \tag{11}$$

where ω_o and η were nondimensional frequency and time parameters, respectively [25]. The shifted and dilated form of the mother wavelet was given by substituting $\frac{t-b}{a}$ for η in (11) [25–28]. For a variety of wavelet scales, (10) can be considered as a series of convolutions between the wavelet function (11) and the original time series for all points. The process was simplified as all convolutions were completed simultaneously for a given scale using the convolution theorem. As such, the wavelet transform was defined as the inverse Fourier transform of the product of the wave function in the Fourier space and the data.

The wavelet spectrum at different frequencies over time was depicted by a contour plot of the wavelet transform with a companion plot of the global spectrum that showed the average variance strength at each frequency. Lastly, to simulate the data, phase randomization, a recent development in wavelet-based simulation methods [7], was applied and compared to auto-regressive and autoregressive integrated moving average (ARIMA) simulations of the wavelet

decomposed energy usage of a DHW heater over the same hour of a day for an entire year. In an effort to fit the data as well as possible, the phase randomization method applied a cosine perturbation to the spectral fit to create an ensemble of DHW heater energy use. Alternative curve fitting techniques were tried and performance compared. A simple auto-regressive process was applied to determine if energy usage could be successfully regressed on its own lagged (i.e., prior) values. In an attempt to improve the auto-regressive fit to the observed energy use, the ARIMA process added (a) a differencing step to accommodate non-stationarity, and (b) a linear combination of error terms for values that occurred contemporaneously and at various times in the past.

To assist in reproducing and extending this work, a representative sample of empirical data and documented R software code can be found in the Supplementary Materials.

4. Results

4.1. Residential Appliance Load Profiles

Stochastic analysis of empirical data revealed diverse, non-normal distributions of energy usage for the studied TCL appliances. In addition, non-stationary usage was indicated by a non-constant mean and variance in different time epochs. The empirical 15-min observations were dominated by zero values and had long tail frequency distributions. Once zero values were removed, kernel density estimates provided insights to bimodal distributions of air conditioner and refrigerator behaviour and trimodal distributions of freezer and hot water heater behaviour. Lastly, spectral methods provided both visualizations of diverse and non-stationary energy usage as well as PDF ensembles of simulated hot water heater behaviour.

The observed energy usage of appliances varied by a factor of 2 or more as depicted in Figure 3, which assumed continual usage on an annual basis. The positive skew in boxplots indicates the presence of high energy-consuming appliances.
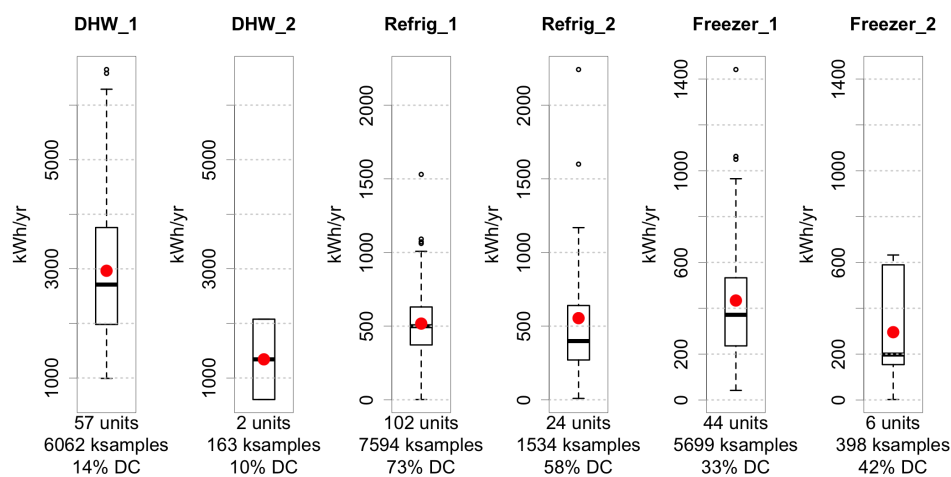

Figure 3. Boxplots of TCL appliance annual energy use. Mean values are shown in red. Values below each plot indicate the number of appliances, sample observations, and average duty cycle from Q2 2012–Q1 2013 inclusive. Note the wide range of diversity, particularly among refrigerators and freezers.

The titles above each boxplot in Figure 3 refer to appliance types, e.g., DWH_1 denotes primary electric hot water heaters. Numerical summaries below each boxplot provided insight into the number of appliances by type in the RBSA data, the number of total observations, and the duty cycle. As expected, all homes had a primary refrigerator. About a quarter of homes had a secondary refrigerator, and almost 40% of homes had a stand-alone freezer. A total of six homes had a secondary freezer and the low the number of samples for this appliance type indicate there were many

NAs in the data, indicating missing observations, perhaps because secondary freezers were not operated year-round.

The diversity in empirical energy consumption impacted the bounds of energy usage for small sets of homes that are typically fed by a split-phase transformer. For example, depending on the number of homes, the mean energy used to heat DHW had wider bounds with fewer homes sampled as depicted in Figure 4.
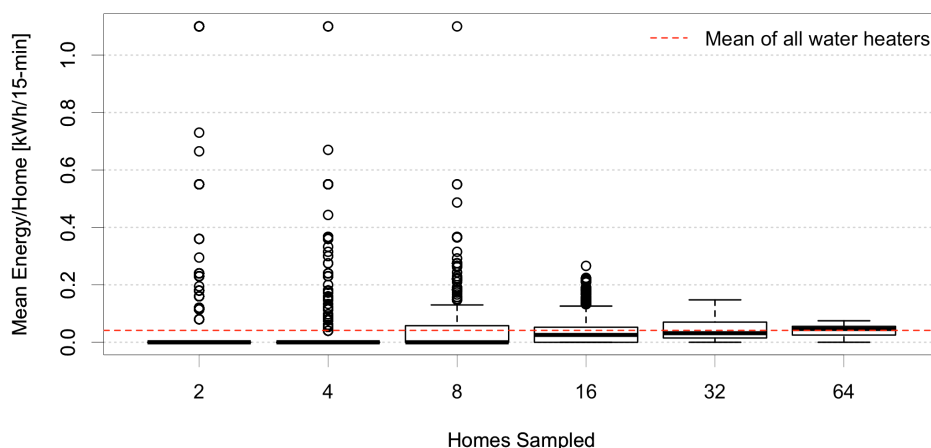

Figure 4. Bounds of electric energy usage for heating DHW over interval 00:00 to 00:15 on 04-01-2012. Moving left to right towards more houses being sampled, note the tighter bounds, fewer outliers, and the median values approaching the mean energy usage of all electric water heaters.

The convergence to mean energy usage in Figure 4 provided an empirical building block for calculating uncertainty in shedding or adding load as a function of the number of participating houses. Simply put, an increase in participating homes resulted in greater certainty in the amount of load that could be shed or added.

Focusing on a single DHW heater, the distributional statistics of energy usage varied at 15-min intervals (5 plots from left to right) and per day (at far right) as depicted in Figure 5.
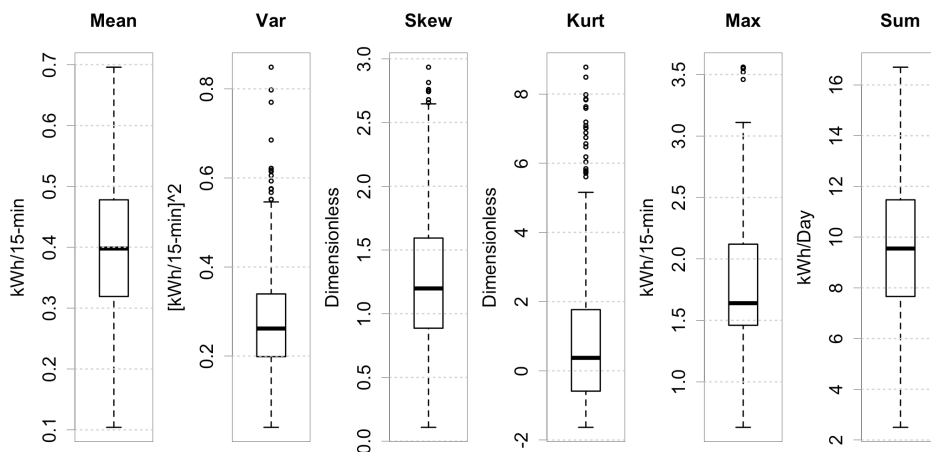
Figure 5. Electric DHW heater energy usage in RBSA home 10388 per 15-min interval and per day from Q2 2012–Q1 2013 inclusive. Usage is representative of observations of electric DHW heaters in other homes.

The spread in Figure 5 statistics provided insight to the diversity in the energy usage of a single appliance, in this case, a DHW heater. Note the daily sum at far right varied by a factor of approximately eight.

Summing DHW heater energy usage into 1-h intervals, an annual distribution of usage by the hour of the day is shown in Figure 6.
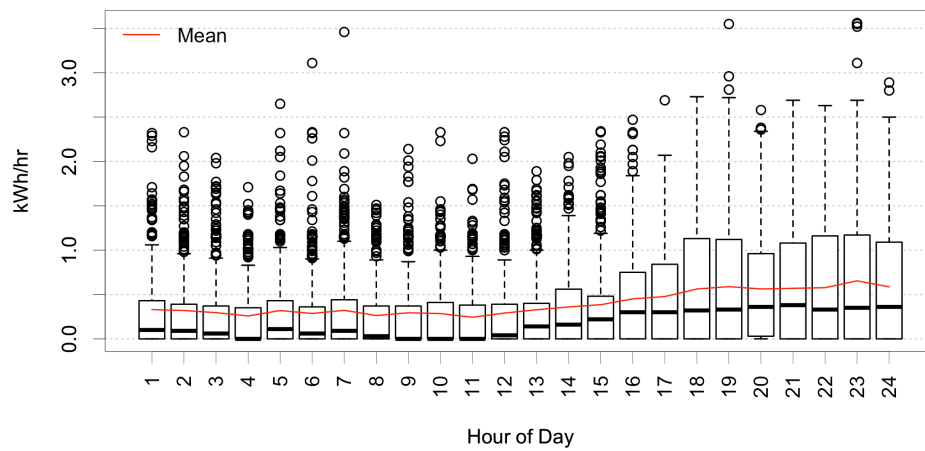

Figure 6. DHW heater energy usage in RBSA home 10388 per hour of day from Q2 2012–Q1 2013 inclusive. Note that there were more outliers but lower interquartile variance in early morning hours.

From Figure 6, it can be inferred that 5 a.m. is the start of increased hot water usage in the morning and is among the high-variance off-peak hours. Hours of high variance can result in difficulties in estimating instantaneous load shed and add opportunities. As such, the 5 a.m. hour was chosen as a difficult test case for evaluating curve fitting and creating simulation ensembles. If 5 a.m. daily energy usage could be simulated for one DHW heater, other hours, water heaters, homes and, cities could be modeled similarly.

The limitations of conventional linear and quadratic curve fitting methods were evident when attempting to capture the energy usage variance shown in Figure 6 and resulted in unsatisfactory curve fits of the time-varying, non-stationary empirical appliance usage data. As a solution test case, the spectral WARM method was applied to decompose and reconstruct the energy usage of DHW heating in the 5 a.m. hour over the course of a year and resulted in a nearly perfect curve fit as depicted in Figure 7 (six months are shown for visual clarity of chart).
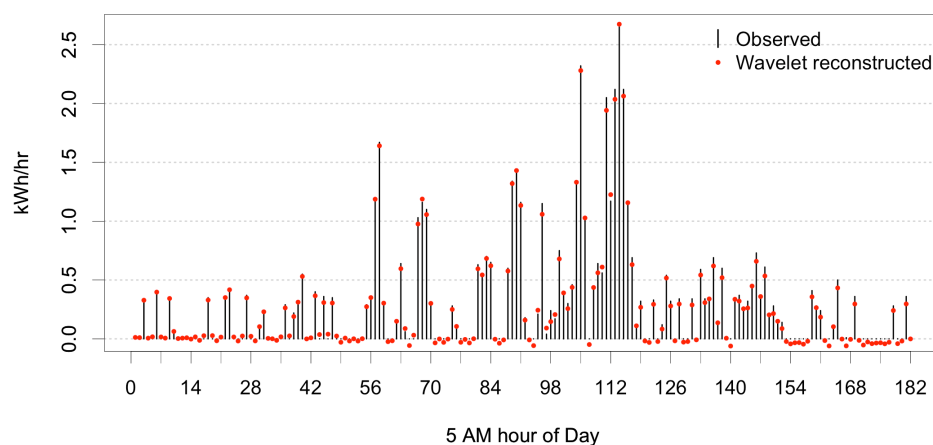
Figure 7. A WARM-based curve fit of 5 a.m. hourly energy usage of DHW heater in RBSA home 10388 from Q2 2012–Q3 2012 inclusive. Prediction errors in the *ON* state are depicted by the vertical offset between the observed value at the top of each bar and its corresponding wavelet reconstructed value denoted as a red dot; errors in the *OFF* states include non-zero values viewed along the day-axis.

4.2. Residential Load Shaping Opportunities

Diversity in appliance empirical energy usage resulted in varying load shaping opportunities across the studied NEEA RBSA homes, of which, 57 homes used electricity to heat DHW and 44 used natural gas or propane. To estimate opportunities at 15-min intervals, (1) and (2) were applied to estimate the ability of individual electric TCL appliances to shed and add load given a look-ahead period of 24-h for L_{max}. Next, on a per home basis, opportunities were summed across TCL appliances by applying (3) and (4) to calculate the lower and upper instantaneous limits of load shaping, as depicted in Figure 8 (six-hours are shown for visual clarity of chart) and Table 2.

First 6 hours of 1 April 2012 at 15-min intervals
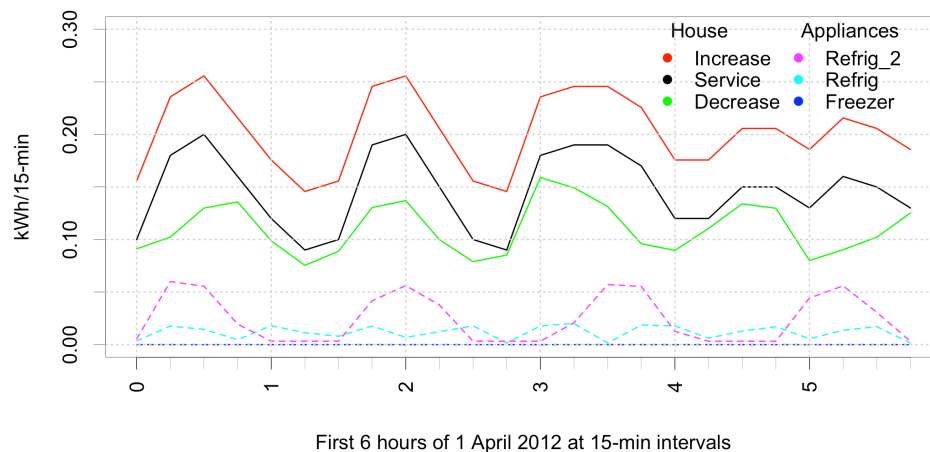
Figure 8. Energy usage profile in 15-min intervals of RBSA home 13019. The black line denotes the electric service for the whole-building. The vertical distance from the black line down to the green line is the instantaneous load that could be shed. The vertical distance from the black line up to the red line is the instantaneous load that could be added. The energy usage of 2 refrigerators and a freezer are depicted by purple, light blue, and dark blue dashed lines at the bottom of the graph. RBSA home 13019 is representative of homes with gas DHW heaters.

Table 2. Load-shaping opportunities across 15-min intervals for Home 13019 for the first six hours during 1 April 2012.

Opportunities	Maximum	Minimum	Mean
Increase load [kW]	0.80	0.36	0.59
Decrease load [kW]	0.64	0.30	0.44

Electricity usage from individual homes was summed using (5) and (6) to estimate the instantaneous load shaping opportunities across groups of homes. Summing the upper and lower limits and the whole-building electric usage across the 14 homes exhibiting best data quality yielded an aggregate instantaneous load that could be shed or added, as depicted in Figure 9 (14 homes were chosen for visual clarity of chart).

Summing across houses showed that, at any point in time, significantly more load could be added than could be shed. This result is primarily attributable to the low duty cycle and the high instantaneous load of DHW heaters, which is on the order of 10 to 40 times greater than that of refrigerators and freezers.
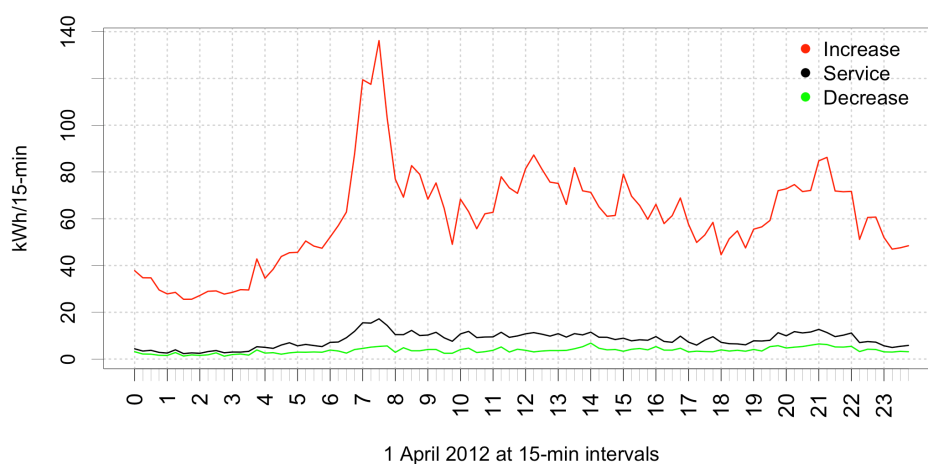
Figure 9. Aggregate load profile of 14 homes at 15-min intervals. The vertical distance from the black line down to the green line is the instantaneous load that could be shed. The vertical distance from the black line up to the red line is the instantaneous load that could be added. The large red spikes indicate significant load adding opportunities, e.g., after completion of morning DHW heating. Greater mid-day and evening load shaping opportunities were also evident.

4.3. Spectral Visualization and Simulation of Appliance Loads

None of the results discussed thus far provide visual insight to time-varying appliance energy usage throughout the year. A major benefit of wavelet visualizations is their ability to convey more comprehensive information than traditional distributional metrics and visualizations such as box plots and histograms. For example, the wavelet-based single DHW heater visualization depicted in Figure 10 was based on 15-min electricity usage over 25 months. In Figure 10, the plot at left is the wavelet-based local power spectrum, the y-axis is the wavelet period, and the x-axis is the wavelet location in time. The colors white and blue denote the lower power spectra. Yellow and red denote the higher power spectra. The arch denotes the "cone of influence" above which there is limited confidence in the data [25]. The graph at the right denotes the global power spectrum as would be found using Fourier analysis. The thin solid and dashed gray lines indicate the 95% and 90% confidence levels given red noise, which has a power spectrum weighted toward low frequencies but has no single preferred period. While both red noise and white noise have zero mean and constant variance, red noise was chosen as it is serially correlated in time, resulting in the lag-1 autocorrelation between two successive time samples having a correlation coefficient, r, such that $0 < r < 1$ [29]. Additional wavelet visualizations of energy usage by RBSA refrigerators and freezers may be found in [6].

Using a nonparametric density estimation technique, spectral reconstruction was used to simulate PDF ensembles of the 5 a.m. energy usage of a DHW heater and were compared to the PDF of the empirical data. There were differing results from the simulations based on wavelet-based phase randomization, straight autoregressive, and ARIMA methods. The phase randomization method applied a cosine perturbation to the spectral fit and exhibited the best performance in creating ensembles of DHW heaters that model the empirical PDF, as depicted in Figure 11.

The straight autoregressive and ARIMA simulation results were obtained using the STATS::ARIMA.SIM Function from the R programming environment [30]. The simulations based on the straight autoregressive method performed similarly to ARIMA simulations, with PDF ensembles from both methods showing poor fits as depicted in Figures 11 and 12.

In both Figures 12 and 13, the simulation ensembles do not reflect the empirical PDF. Also, note the high occurrence of unrealistic negative values further indicating poor curve fits by the straight autoregressive and ARIMA simulation methods.
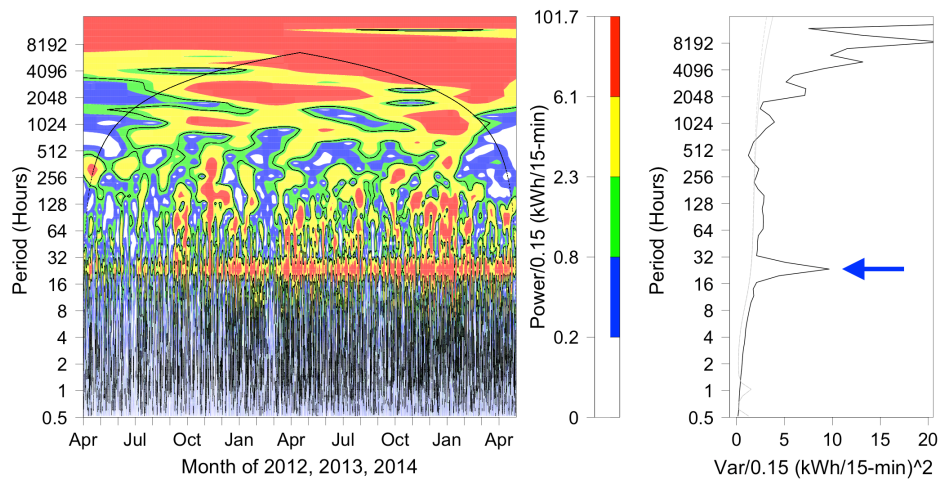
Figure 10. Plots for the DHW heater in RBSA home 22284, from April 2012–April 2014 inclusive. At left, red denotes periods of greater hot water use. Red along the 24-h period indicates sustained diurnal use, which is also shown in the companion graph at right by the peak next to the left arrow. Less red at far left indicates less hot water was used in the 24-hour (and greater periods) from April through September 2012. Non-stationary usage was also observed in other homes and appliances.
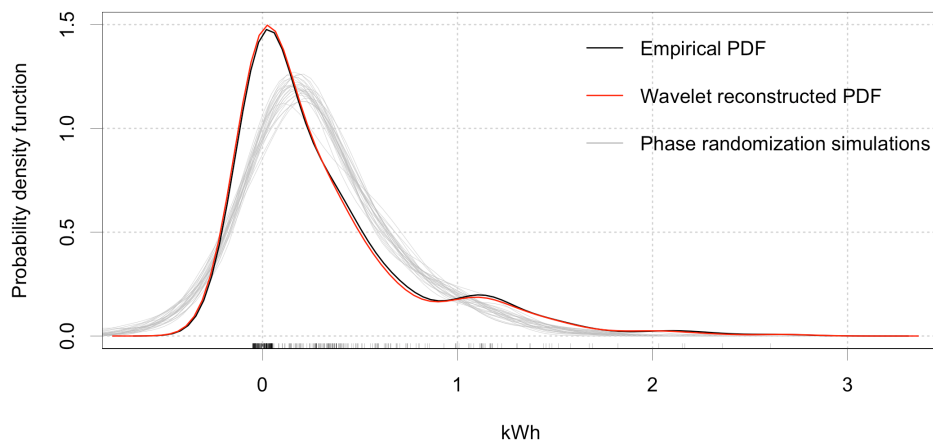

Figure 11. Simulation of the wavelet decomposed 5 a.m. hourly energy usage by DHW heater in RBSA home 13088 from Q2 2012–Q1 2013 inclusive, using the *phase randomization* method.
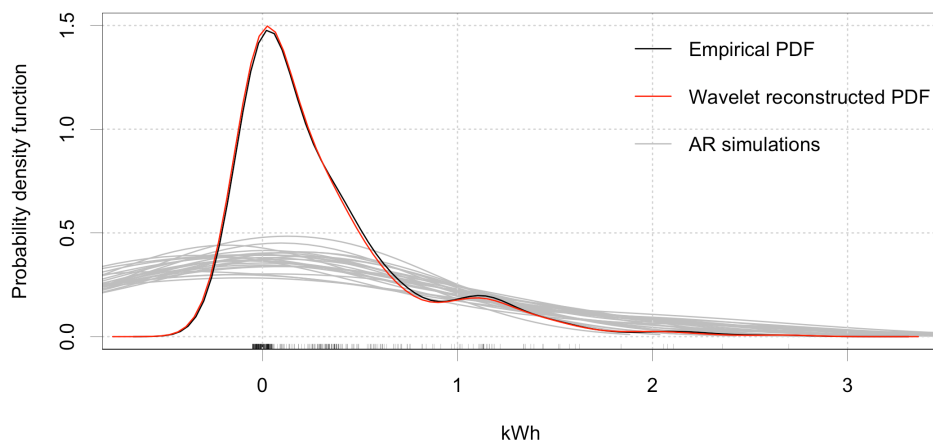
Figure 12. Simulation of the wavelet decomposed 5 a.m. hourly energy usage by DHW heater in RBSA home 13088 from Q2 2012–Q1 2013 inclusive, using the *Autoregressive* method.
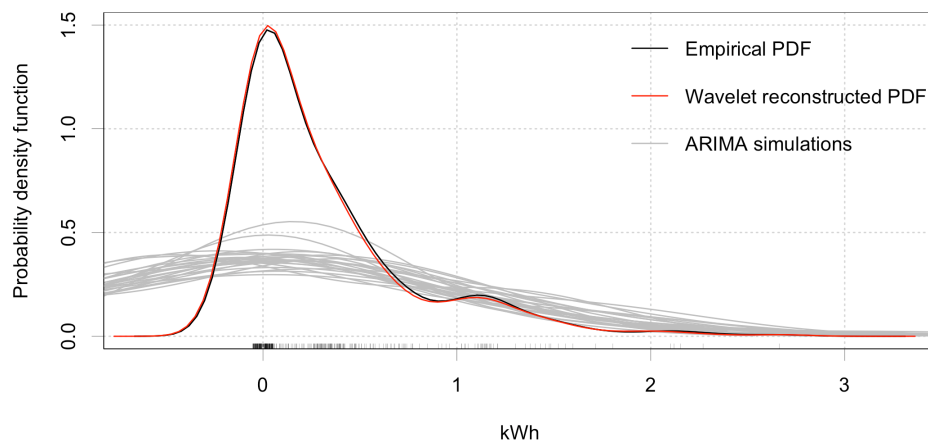
Figure 13. Simulation of the wavelet decomposed 5 a.m. hourly energy usage by DHW heater in RBSA home 13088 from Q2 2012–Q1 2013 inclusive, using the *ARIMA* method.

Figure 14 summarizes the PDF ensembles in Figures 11 and 12 as boxplots. The phase randomization method most accurately modeled the observed behaviour of the empirical PDF.
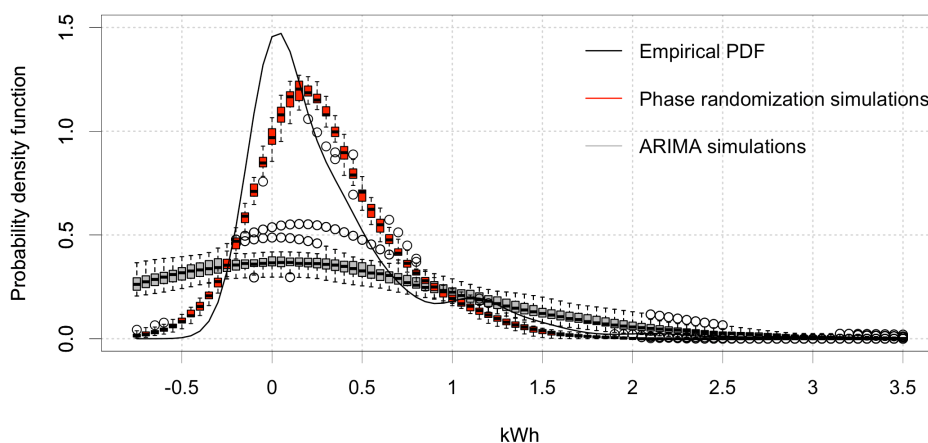

Figure 14. Comparison of phase randomization and ARIMA simulation techniques of the wavelet decomposed 5 a.m. hourly energy usage by DHW heater in RBSA home 13088 from Q2 2012–Q1 2013 inclusive.

To quantify the performance of the simulation methods, distributional statistics for the first, second, third and fourth statistical moments (mean, variance, skew, and kurtosis) were shown for all simulations, along with maximum, minimum and sum, in Figures 15–17. For comparison, the performance of each simulation method was shown along with statistics from the empirical observations. For most statistical measures, the phase randomization method had better simulation performance than either the straight autoregressive or ARIMA methods.

Note in Figure 15, the unrealistic slightly negative mean energy usage and spread in the variance of both the straight autoregressive and ARIMA simulation methods.

In Figure 16, the statistics of all simulation methods were less than in the observed RBSA data.

Figure 17 further highlights the challenges in simulating RBSA appliance usage data, in this case, for a single DHW heater. Note that all simulation methods understated both peak usage and minimum usage, some more so than others. Figures 15–17 together highlight the limitations in all simulation methods and quantify the superior performance of phase randomization over both the straight autoregressive and ARIMA simulation methods.

In summary, results indicate the ability for different types of Internet-connected appliances to shed and add electric load throughout the day. The implications of automatically adding and shedding loads are significant in the context of the grid supporting increased penetration of RES [8–10]. Results also indicate the improved performance of spectral methods over traditional statistical methods in the ability to quantify and simulate non-stationary behavior [7], which addresses concerns in the literature of preserving energy use diversity [5] and improving model fidelity [4] for realistic simulation of the generation-to-load system-level response.
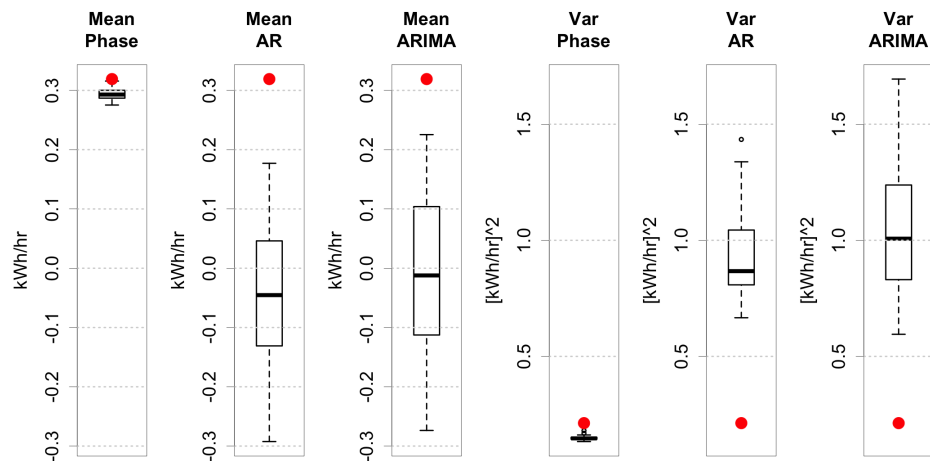
Figure 15. Boxplots of mean and variance comparing the performance of reconstruction methods in simulating the 5 a.m. hourly energy usage by the electric DHW heater in RBSA home 13088, from Q2 2012–Q1 2013 inclusive. Statistics of empirical observations are denoted by red dots. For mean and variance, phase randomization provided superior performance.
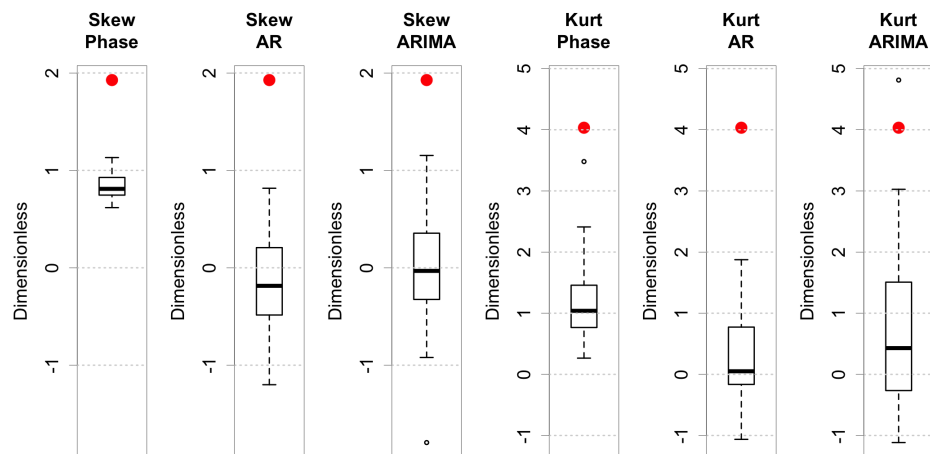

Figure 16. Boxplots of skew and kurtosis comparing the performance of reconstruction methods in simulating the 5 a.m. hourly energy usage by the electric DHW heater in RBSA home 13088, from Q2 2012–Q1 2013 inclusive. Statistics of empirical observations are denoted by red dots. For skew and kurtosis, the phase randomization method had somewhat better performance.
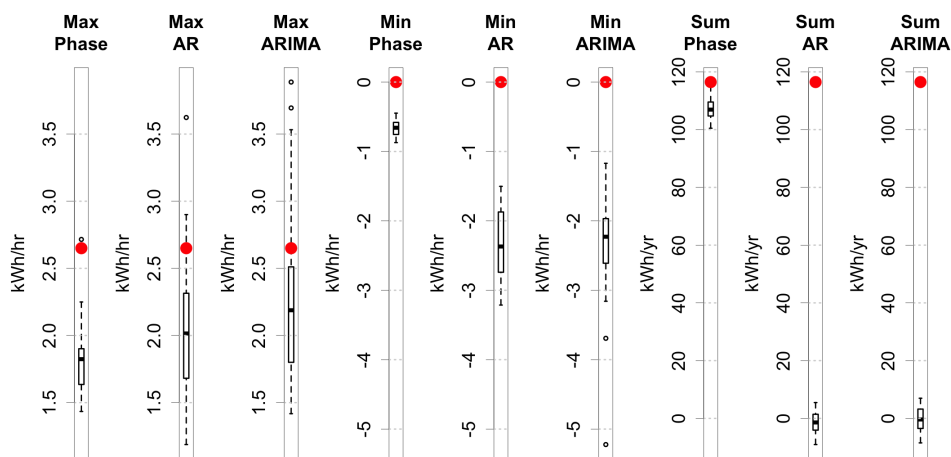
Figure 17. Boxplots of maximum, minimum and sum compared the performance of reconstruction methods in simulating the 5 a.m. hourly energy usage by the electric DHW heater in RBSA home 13088, from Q2 2012–Q1 2013 inclusive. Statistics of empirical observations are denoted by red dots. Note: (a) the significant variances in the maximum statistic would adversely affect load shaping calculations, (b) the minimum statistic included unrealistic negative values, and (c) Mean values of zero in the AR and ARIMA sum statistics were unrealistic.

5. Conclusions and Outlook for Future Work

In this study, it was assumed that utilities would evolve beyond direct load control and use automated residential load shaping (ARLS) to create elasticity in demand by continually broadcasting a forecast dynamic price of electricity to IoT appliances in order to maximize generation efficiency and minimize the cost of electric power production and consumption. Changes in pricing resulted in instantaneous load shed and add opportunities which were quantified for single-family homes in the Northwest United States. Empirical appliance energy use data were explored across individual homes and groups of homes resulting in several interesting features and statistics, including the correlation between duty cycle and instantaneous opportunities, however brief they might be, to shed or add electric load.

Wavelet-based spectral analysis was use to capture, view, and simulate diverse and unknown drivers of load such as the type, age, and time of use of appliances and occupancy characteristics. The performance of WARM phase randomization, auto-regressive and ARIMA simulation methods were compared; the ability of each method to reflect diversity in energy usage of an actual DHW water heater in a high variance hour over the course of a year was quantified, with phase randomization providing the most accurate simulation ensembles. Most importantly, this work provided insights in quantifying diversity in appliance energy consumption—without *a priori* knowledge of appliance details—and in simulating load ensembles that reflect observed energy use. The main contribution is that a robust simulation technique like WARM provides the ability to simulate synthetic subdivisions for use in energy management research. The WARM can be used to simulate a variety of ensembles mimicking each appliance in a subdivision in order to aggregate statistics of energy usage, by house and electrical distribution feeder, for potential decision making in managing the grid.

In related research, ARLS was extended to explore the potential for shaping demand at the distribution feeder level in order to maximize the use of RES and minimize variable electricity generation costs. A physical model of the interaction between electric loads and building thermal mass was used to simulate interior building temperatures and air conditioning behaviour, subject to occupant comfort constraints. Location-specific weather and region-specific residential building envelopes were inputs to the model. Instantaneous load-shedding and load-adding opportunities were quantified for greater than 100,000 individual homes. Location-specific weather was used to simulate electric loads on 204 electrical distribution feeders with load shed and add results presented for 35 cities

across the United States [22]. In the future application of this work, in the context of distributed model predictive control [31,32], ARLS is further expanded and coupled to electricity production cost models to jointly minimize financial costs for large geographical regions encompassing several IECC climate zones [33] in the United States. Financial costs to be minimized are the production operations of utility-scale thermal and renewable generation, by modifying the charging and discharging behaviour of residential batteries, the heating of DHW, and the cooling of residential buildings with central air conditioning.

References

1.　Florida Power and Light. On Call. Available online: https://www.fpl.com/save/pdf/oncall.pdf (accessed on 8 June 2019).

2.　Fell, M.J.; Shipworth, D.; Huebner, G.M.; Elwell, C.A. Public acceptability of domestic demand-side response in Great Britain: The role of automation and direct load control. *Energy Res. Soc. Sci.* **2015**, *9*, 72–84, doi:10.1016/j.erss.2015.08.023.

3.　Hu, Z.; Kim, J.H.; Wang, J.; Byrne, J. Review of dynamic pricing programs in the U.S. and Europe: Status quo and policy recommendations. *Renew. Sustain. Energy Rev.* **2015**, *42*, 743–751, doi:10.1016/j.rser.2014.10.078.

4.　McKenna, K.; Keane, A. Residential Load Modeling of Price-Based Demand Response for Network Impact Studies. *IEEE Trans. Smart Grid* **2016**, *7*, 2285–2294, doi:10.1109/tsg.2015.2437451.

5.　Ramírez-Mendiola, J.L.; Grünewald, P.; Eyre, N. The diversity of residential electricity demand—A comparative analysis of metered and simulated data. *Energy Build.* **2017**, *151*, 121–131, doi:10.1016/j.enbuild.2017.06.006.

6.　Cruickshank, R.F.; Henze, G.P.; Balaji, R.; Hodge, B.-M.S.; Florita, A.R. Empirical Investigations of the Opportunity Limits of Automatic Residential Electric Load Shaping. In Proceedings of the 9th Annual IEEE Green Technologies Conference, Denver, CO, USA, 30 March 2017, doi:10.1109/greentech.2017.17.

7.　Nowak, K.C.; Rajagopalan, B.; Zagona, E. Wavelet Auto-Regressive Method (WARM) for multi-site streamflow simulation of data with non-stationary spectra. *J. Hydrol.* **2011**, *410*, 1–12, doi:10.1016/j.jhydrol.2011.08.051.

8.　GE Energy. *Western Wind and Solar Integration Study*; Technical Report NREL/SR-550-47434; National Renewable Energy Laboratory: Golden, CO, USA, 2010; doi:10.2172/981991.

9.　Lew, D.; Brinkman, G.; Ibanez, E.; Hodge, B.-M.; Hummon, M.; Florita, A.; Heaney, M. *Western Wind and Solar Integration Study Phase 2*; Technical Report NREL/TP-5500-55588; National Renewable Energy Laboratory: Golden, CO, USA, 2013; doi:10.2172/1095399.

10.　Miller, N.W.; Shao, M.; Pajic, S.; D'Aquila, R. *Western Wind and Solar Integration Study Phase 3-Frequency Response and Transient Stability*; Technical Report NREL/SR-5D00-62906; National Renewable Energy Laboratory: Golden, CO, USA; GE Energy Management: Schenectady, NY, USA, 2014; doi:10.2172/1167065.

11.　Chassin, D.P.; Posse, C. Evaluating North American electric grid reliability using the Barabási-Albert network model. *Phys. A Stat. Mech. Appl.* **2005**, *355*, 667–677, doi:10.1016/j.physa.2005.02.051.

12. Beér, J.M. High efficiency electric power generation: The environmental role. *Prog. Energy Combust. Sci.* **2007**, *33*, 107–134, doi:10.1016/j.pecs.2006.08.002.

13. Henbest, S. New Energy Outlook 2018: Bloomberg's Annual Long-Term Economic Analysis of the World's Power Sector out to 2050. Presented at the Bloomberg New Energy Finance Summit, New York, NY, USA, 9–10 April 2018. Available online: https://bnef.turtl.co/story/neo2018?teaser=truef (accessed on 8 June 2019).

14. Verbruggen, A.; Lauber, V. Basic concepts for designing renewable electricity support aiming at a full-scale transition by 2050. *Energy Policy* **2009**, *37*, 5732–5743, doi:10.1016/j.enpol.2009.08.044.

15. Darby, S.J.; McKenna, E. Social implications of residential demand response in cool temperate climates. *Energy Policy* **2012**, *49*, 759–769, doi:10.1016/j.enpol.2012.07.026.

16. Hirth, L. The market value of variable renewables. *Energy Econ.* **2013**, *38*, 218–236, doi:10.1016/j.eneco.2013.02.004.

17. Nicolosi, M.; Fürsch, M. The Impact of an increasing share of RES-E on the Conventional Power Market—The Example of Germany. *Z. Energ.* **2009**, *33*, 246–254, doi:10.1007/s12398-009-0030-0.

18. Boßmann, T.; Eser, E.J. Model-based assessment of demand-response measures—A comprehensive literature review. *Renew. Sustain. Energy Rev.* **2016**, *57*, 1637–1656, doi:10.1016/j.rser.2015.12.031.

19. Elghitani, F.; Zhuang, W. Aggregating a Large Number of Residential Appliances for Demand Response Applications. *IEEE Trans. Smart Grid* **2018**, *9*, 5092–5100, doi:10.1109/tsg.2017.2679702.

20. Northwest Energy Efficiency Alliance. Residential Building Stock Assessment: Metering Data. 2014. Available online: https://neea.org/data/residential-building-stock-assessment (accessed on 8 June 2019).

21. Larson, B.; Gilman, L.; Davis, R.; Logsdon, M.; Uslan, J.; Hannas, B.; Baylon, D.; Storm, P.; Mugford, V.; Kvaltine, N. Residential Building Stock Assessment: Metering Study, Northwest Energy Efficiency Alliance. 2014. Available online: https://neea.org/img/documents/residential-building-stock-assessment-metering-study.pdf (accessed on 7 June 2019).

22. Cruickshank, R.F.; Florita, A.R.; Henze, G.P.; Corbin, C.D. Characterizing electric grid system benefits of MPC-based residential load shaping. In Proceedings of the 2018 Building Performance Analysis Conference and SimBuild, Co-Organized by ASHRAE and IBPSA-USA, Chicago, IL, USA, 26–28 September 2018; pp. 791–798.

23. Balaji, R. *CVEN 6833 Class Lecture, Frequency Domain Analysis: Wavelet Spectral Methods for Computing Spectrum of Time Series, and Time Series Simulation Using Spectrum-Wavelet + AR Based Approach*; Department of Civil, Environmental and Architectural Engineering, University of Colorado: Boulder, CO, USA, 2017. Available online: http://civil.colorado.edu/%7Ebalajir/CVEN6833/course-outline-6833-Fall18.pdf (accessed on 8 June 2019).

24. Kwon, H.H.; Lall, U.; Khalil, A.F. Stochastic simulation model for nonstationary time series using an autoregressive wavelet decomposition: Applications to rainfall and temperature. *Water Resour. Res.* **2007**, *43*, doi:10.1029/2006wr005258.

25. Torrence, C.; Compo, G.P. A Practical Guide to Wavelet Analysis. *Bull. Am. Meteorol. Soc.* **1998**, *79*, 61–78, doi:10.1175/1520-0477(1998)079<0061:apgtwa>2.0.co;2.

26. Addison, P. *The Illustrated Wavelet Transform Handbook*; Taylor & Francis: New York, NY, USA, 2002.

27. Kwon, H.H.; Lall, U.; Obeysekera, J. Simulation of daily rainfall scenarios with interannual and multidecadal climate cycles for South Florida. *Stoch. Environ. Res. Risk Assess.* **2009**, *23*, 879–896, doi:10.1007/s00477-008-0270-2.

28. Torrence, C.; Webster, P.J. The annual cycle of persistence in the El Niño/Southern Oscillation. *Q. J. R. Meteorol. Soc.* **1998**, *124*, 1985–2004, doi:10.1002/qj.49712455010.

29. Hartmann, D. *ATMS 552 Class Notes, Time Series Analysis-Section 6a, Statistical Prediction, Red and White Noise*; Department of Atmospheric Sciences, College of Environment, University of Washington: Seattle, WA, USA, 2014. Available online: https://atmos.uw.edu/~dennis/552_Notes_6a.pdf (accessed on 8 June 2019).

30. R Core Team. *R: A Language and Environment for Statistical Computing*; R Foundation for Statistical Computing: Vienna, Austria, 2018.

31. Corbin, C.; Henze, G. Predictive control of residential HVAC and its impact on the grid. Part I: Simulation framework and models. *J. Build. Perform. Simul.* **2017**, *10*, 294–312, doi:10.1080/19401493.2016.1231220.

32. Corbin, C.; Henze, G. Predictive control of residential HVAC and its impact on the grid. Part II: Simulation studies of residential HVAC as a supply following resource. *J. Build. Perform. Simul.* **2017**, *10*, 365–377, doi:10.1080/19401493.2016.1231221.

33. International Code Council. Climate Zone Map. Available online: https://www2.iccsafe.org/states/Phoenix2006/Phoenix_Energy/PDFs/Chapter3_ClimateZones.pdf (accessed on 5 August 2018).